Available online at www.sciencedirect.com
SCIENCE DIRECT®
ELSEVIER
Nuclear Instruments and Methods in Physics Research B 221 (2004) 149–159
NIM B
Beam Interactions with Materials & Atoms
www.elsevier.com/locate/nimb

Positronium–atom collisions

H.R.J. Walters, A.C.H. Yu *, S. Sahoo, Sharon Gilmore

Department of Applied Mathematics and Theoretical Physics, Queen's University, Belfast BT7 1NN, United Kingdom

Abstract

New results are presented for Ps(1s) scattering by H(1s), He(1^1S) and Li(2s). Calculations have been performed in a coupled state framework, usually employing pseudostates, and allowing for excitation of both the Ps and the atom. In the Ps(1s)–H(1s) calculations the H^- formation channel has also been included using a highly accurate H^- wave function. Resonances resulting from unstable states in which the positron orbits H^- have been calculated and analysed. The new Ps(1s)–He(1^1S) calculations still fail to resolve existing discrepancies between theory and experiment at very low energies. The possible importance of the Ps^- formation channel in all three collision systems is discussed.

PACS: 34.50.−s; 36.10.Dr
Keywords: Positronium; Scattering; Close coupling; Pseudostates; Atomic hydrogen; Helium; Lithium; Alkali metal; Resonances; Positronium negative ion; Hydrogen negative ion

1. Introduction

In this article we present some new theoretical results for positronium(Ps)–atom scattering for three fundamental systems: Ps–H, Ps–He and Ps–alkali metal, taking Li as our example of an alkali metal. In each case we assume that the incident Ps and the target atom are both in their ground states. Throughout we use atomic units (au) in which $\hbar = m_e = e = 1$, the symbol a_0 is used to denote the Bohr radius, $a_0 = \hbar^2/me^2$. To express energies derived in atomic units, e.g., the calculated position and width of a resonance, in electron volts (eV) we have used the conversion 1 au = 27.21138344(106) eV [1].

* Corresponding author.
E-mail addresses: h.walters@qub.ac.uk (H.R.J. Walters), a.yu@qub.ac.uk (A.C.H. Yu), s.sahoo@qub.ac.uk (S. Sahoo), s.gilmore@qub.ac.uk (S. Gilmore).

2. Positronium scattering by atomic hydrogen (Ps(1s)–H(1s))

2.1. Event line

Fig. 1 shows an event line for this system. In a non-relativistic treatment of Ps–H collisions the total electronic spin, S_e, is conserved. Since the system contains two electrons the possible values of S_e are 0 and 1. Fig. 1 illustrates the case of scattering in the electronic spin singlet state $S_e = 0$. From Fig. 1 we see that the system possesses a single S-wave bound state [2], positronium hydride (PsH), with a binding energy of 1.0666 eV [3]. As far as scattering is concerned, the significance of this bound state is that it corresponds mathematically to a pole at an impact energy of −1.0666 eV in the S-wave singlet scattering amplitude. As we approach zero impact energy the singlet elastic cross section, which becomes increasingly S-wave,

0168-583X/$ - see front matter
doi:10.1016/j.nimb.2004.03.047

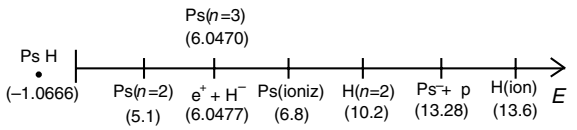

Fig. 1. Event line for Ps(1s)–H(1s) scattering in the electronic spin singlet state. Events are shown as a function of the impact energy E (in eV). The diagram is purely schematic and not to scale.

rises towards the pole, see Fig. 2. The precise value of the zero energy singlet cross section in a calculation therefore depends upon how well this pole is represented.

Up until 5.1 eV only elastic Ps(1s)–H(1s) scattering is possible. At 5.1 eV Ps ($n = 2$) excitation becomes feasible, the atom still remaining in its ground state. At 6.0470 eV Ps ($n = 3$) excitation comes on line. Interestingly, this threshold is almost coincident with that for H^- formation ($Ps + H \Rightarrow H^- + e^+$) at 6.0477 eV [4]. In quoting these numbers we have ignored relativistic effects and have assumed that the proton has infinite mass. One wonders whether this near degeneracy might present some interesting experimental opportunities. Certainly, it should lead to a competition between the two channels and since, as we shall see later (Fig. 3), there is a rich Rydberg resonance structure associated with the H^- threshold, it presumably has some effect upon this structure.

Between 6.0477 and 6.8 eV the full Rydberg spectrum of Ps becomes accessible until, at last, at

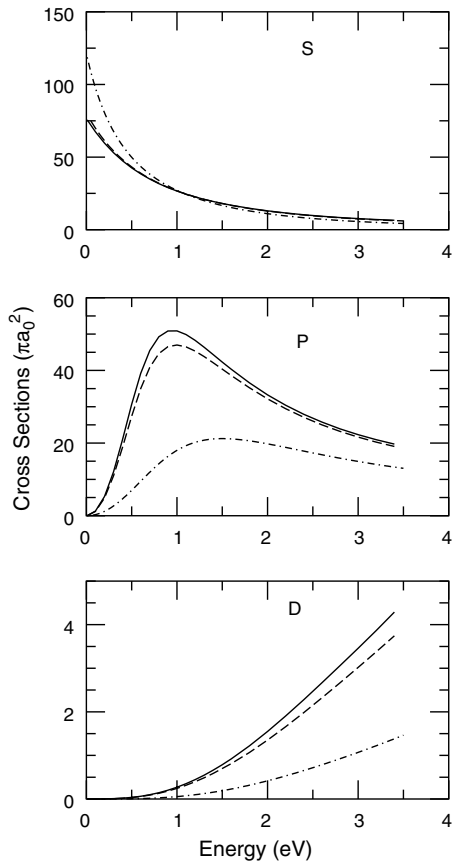

Fig. 2. Electronic spin singlet partial wave cross sections for Ps(1s)–H(1s) elastic scattering in the energy range 0–3.5 eV. Approximations: solid curve, 9Ps9H + H⁻; dashed curve, 9Ps9H; dash–dot curve, 9Ps1H.

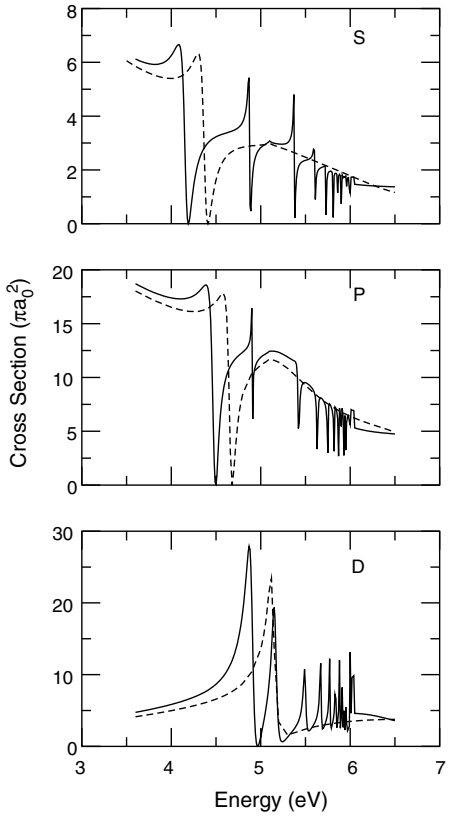

Fig. 3. Electronic spin singlet partial wave cross sections for Ps(1s)–H(1s) elastic scattering in the energy range 3.5–6.5 eV. Approximations: solid curve, 9Ps9H + H⁻; dashed curve, 9Ps9H.

6.8 eV the Ps can be ionized. Not until 10.2 eV can the atom be excited, to the $n = 2$ level with the Ps remaining in its ground state. Ionization of the atom becomes possible at 13.6 eV. However, between 10.2 and 13.6 eV another interesting threshold appears, Ps^- formation ($Ps + H \Rightarrow Ps^- + p$), at 13.28 eV [4]. This threshold lies in the midst of thresholds for producing highly excited H (in fact between the H ($n = 6$) and H ($n = 7$) thresholds). As with H^- we would expect Rydberg resonance structure associated with the Ps^- threshold, although probably much less pronounced.

Beyond the energy range of Fig. 1, double excitation of both projectile and target becomes possible at 15.3 eV and double ionization at 20.4 eV.

Scattering in the electronic spin triplet ($S_e = 1$) channels is somewhat less interesting, although usually the dominant component of any spin averaged cross section. The event line for triplet scattering is the same as Fig. 1 except that the PsH bound state and the H^- and Ps^- channels are omitted. The absence of these formation channels means also a corresponding absence of resonance structure.

2.2. Coupled pseudostate calculations

The challenge to theory is to represent the events portrayed in Fig. 1 in an adequate way. A suitable and powerful representation is provided by the coupled pseudostate approach.

Let $\mathbf{r}_p(\mathbf{r}_i)$ be the position vector of the positron (ith electron) relative to the proton, which is assumed to be infinitely massive. $\mathbf{R}_i \equiv (\mathbf{r}_p + \mathbf{r}_i)/2$ and $\mathbf{t}_i \equiv (\mathbf{r}_p - \mathbf{r}_i)$ then correspond to the centre of mass of the Ps relative to the proton and to the Ps internal coordinate when the Ps consists of the positron and the ith electron. The non-relativistic Hamiltonian for the Ps–H system is then

$$H = -\frac{1}{4}\nabla^2_{R_1} + H_{Ps}(\mathbf{t}_1) + H_A(\mathbf{r}_2) + \frac{1}{r_p} - \frac{1}{r_1} - \frac{1}{|\mathbf{r}_p - \mathbf{r}_2|} + \frac{1}{|\mathbf{r}_1 - \mathbf{r}_2|}, \quad (1)$$

where

$$H_{Ps}(\mathbf{t}) \equiv -\nabla^2_t - \frac{1}{t} \quad (2)$$

is the Hamiltonian for Ps and

$$H_A(\mathbf{r}) \equiv -\frac{1}{2}\nabla^2_r - \frac{1}{r} \quad (3)$$

is the Hamiltonian for atomic hydrogen. The Hamiltonian (1) is, of course, unchanged by the interchange $\mathbf{r}_1 \leftrightarrow \mathbf{r}_2$.

Following previous work [5,6] we expand the collisional wave function, Ψ, for the system in a particular state of total electronic spin S_e according to

$$\Psi = \sum_{a,b}\Big[G_{ab}(\mathbf{R}_1)\phi_a(\mathbf{t}_1)\psi_b(\mathbf{r}_2) + (-1)^{S_e}G_{ab}(\mathbf{R}_2)\phi_a(\mathbf{t}_2)\psi_b(\mathbf{r}_1)\Big], \quad (4)$$

where the sum is over Ps states ϕ_a and H states ψ_b. These states may be either eigenstates or pseudostates and have the property that

$$\langle\phi_a(\mathbf{t})|H_{Ps}(\mathbf{t})|\phi_{a'}(\mathbf{t})\rangle = E_a\delta_{aa'}, \quad \langle\phi_a(\mathbf{t})|\phi_{a'}(\mathbf{t})\rangle = \delta_{aa'},$$
$$\langle\psi_b(\mathbf{r})|H_A(\mathbf{r})|\psi_{b'}(\mathbf{r})\rangle = \varepsilon_b\delta_{bb'}, \quad \langle\psi_b(\mathbf{r})|\psi_{b'}(\mathbf{r})\rangle = \delta_{bb'}. \quad (5)$$

Substituting (4) into the Schrödinger equation with the Hamiltonian (1) and projecting with $\phi_a(\mathbf{t}_1)\psi_b(\mathbf{r}_2)$ leads to coupled equations for the functions G_{ab} of the form

$$(\nabla^2_{R_1} + p^2_{ab})G_{ab}(\mathbf{R}_1) = 4\sum_{a'b'}V_{ab,a'b'}(\mathbf{R}_1)G_{a'b'}(\mathbf{R}_1) + 4(-1)^{S_e}\sum_{a'b'}\int L_{ab,a'b'}(\mathbf{R}_1,\mathbf{R}_2)G_{a'b'}(\mathbf{R}_2)\,d\mathbf{R}_2. \quad (6)$$

In (6), p_{ab} is the momentum of the Ps in the ab channel, $V_{ab,a'b'}$ gives the direct Coulombic interaction between the Ps and the H atom and $L_{ab,a'b'}$ accounts for electron exchange between Ps and H. The coupled equations (6) are converted to partial wave form and solved using the R-matrix technique [7].

The approximation (4) has been employed in [6] using 9 Ps states and 9 H states, called the 9Ps9H approximation, and, for S-wave scattering only, using 14 Ps and 14 H states (14Ps14H approximation). The 9 states are shown in Table 1, a more detailed specification is given in [6]. They consist of

Table 1
The 9 Ps and 9 H states of the 9Ps9H approximation of [6]

State	Energy (eV)	
	Ps	H
1s	0.0	0.0
2s, 2p	5.1	10.2
$\overline{3}$s, $\overline{3}$p, $\overline{3}$d	6.8	13.6
$\overline{4}$d	13.2	26.5
$\overline{4}$p	13.9	27.9
$\overline{4}$s	17.1	34.2

The energies are as defined in (5).

1s, 2s, 2p eigenstates and $\overline{3}$s, $\overline{3}$p, $\overline{3}$d, $\overline{4}$s, $\overline{4}$p, $\overline{4}$d pseudostates (pseudostates are denoted by a "bar"). The pseudostates give a representation of the Ps/H continua as well as giving an average approximation to the bound eigenstates with $n \geqslant 3$ (the $n = 3$ pseudostates of Table 1 have approximately a 2/3 overlap with the $n \geqslant 3$ eigenstate spectrum [8]). While the 9Ps9H and 14Ps14H approximations should be satisfactory for describing electronic spin triplet scattering, it has been shown in [9], but only within the context of the frozen target approximation, that the e^+–H^- channel exerts a profound effect upon singlet scattering. Here we try to improve upon the earlier calculations of [6] for singlet scattering by explicitly adding on the e^+–H^- channel, our approximation (4) for singlet scattering is then extended to

$$\Psi = \sum_{a,b} \Big[G_{ab}(\mathbf{R}_1)\phi_a(\mathbf{t}_1)\psi_b(\mathbf{r}_2) + (-1)^{S_e} G_{ab}(\mathbf{R}_2)\phi_a(\mathbf{t}_2)\psi_b(\mathbf{r}_1) \Big] + F(\mathbf{r}_p)\psi^-(\mathbf{r}_2,\mathbf{r}_2), \quad (7)$$

where ψ^- is the H^- wave function. We refer to this as the 9Ps9H + H^- or 14Ps14H + H^- approximation, etc., depending upon the number of Ps and H states used in the sum. For ψ^- we have used a highly accurate 100 term Kinoshita–Koga type wave function [10,11] giving an H^- binding energy of 0.0277510163 au. It should be noted that the calculation of [9] was restricted not only by the frozen target approximation but also by the use of an approximate H^- wave function, these restrictions have now been lifted in the present work.

Table 2
PsH bound state

Approximation	Binding energy (eV)
9Ps1H	0.543
9Ps9H	0.963
14Ps14H	0.994
9Ps9H + H^-	1.02
14Ps14H + H^-	1.03
Accurate result of [3]	1.0666

The first test of the approximation (7) is how well it reproduces the PsH binding energy. Table 2 shows the present and earlier calculations compared with the very accurate result of [3]. Here we see that the frozen target approximation 9Ps1H gives only half of the binding energy. The allowance for virtual target excitation in the 9Ps9H and 14Ps14H approximations raises this to 90–93%. Inclusion of the e^+–H^- channel brings further improvement, as we would expect, but our best result, 14Ps14H + H^-, still remains 3.4% below the accurate value of [3]. We estimate that our numerical methods are good enough to yield an answer correct to better than 1%. The deviation of 3.4% from the accurate result of [3] is therefore significant. What is missing? The approximation (7) should represent satisfactorily correlation in which one electron is associated primarily with the proton and the other electron with the positron (the sum in (7)) and in which the two electrons are strongly correlated in association with the proton while the positron moves more freely around this complex (the ψ^- term). What is absent is correlation in which the two electrons and the positron are associated in a strongly correlated unit moving in the field of the proton, in short, a Ps^- structure orbiting the proton. We speculate that the addition of the Ps^- + p channel to (7) might lead to significant improvement.

Recent accurate low energy S-wave calculations by Van Reeth and Humberston [12] using the Kohn variational principle present a further opportunity to test our approximations. In Table 3 we make a comparison of our best calculations for the S-wave singlet phase shifts and scattering length with these accurate numbers. We see that inclusion of the $e^+ + H^-$ channel roughly halves the difference between the 14Ps14H approximation

Table 3
S-wave phase shifts (in rad) and scattering length for electronic spin singlet Ps(1s)–H(1s) scattering

Incident momentum (au)	14Ps14H	14Ps14H + H^-	Van Reeth and Humberston [12]
0.1	−0.434	−0.428	−0.425
0.2	−0.834	−0.825	−0.817
0.3	−1.178	−1.167	−1.158
0.4	−1.467	−1.453	−1.443
0.5	−1.704	−1.685	−1.674
0.6	−1.890	−1.867	−1.852
0.7	−2.018	−1.992	−1.959
Scattering length (au)	4.41	4.327	4.311

and the variational results for the phase shifts. With the exception of the last point at 0.7 au, our best phase shifts, in the 14Ps14H + H^- approximation, now differ from the variational numbers by about 1%. The agreement between the 14Ps14H + H^- scattering length and the variational answer is particularly good.

The largest calculation that we have made for higher partial waves is in the 9Ps9H + H^- approximation. In Table 4 we list the phase shifts in this approximation for S-, P-, D-wave scattering. Comparing Tables 3 and 4, we see that the S-wave phase shifts in the 9Ps9H + H^- approximation are only marginally better than those in the 14Ps14H approximation which does not include the e^+–H^- channel.

Fig. 2 shows S, P and D electronic spin singlet elastic partial wave cross sections in the energy range 0–3.5 eV. The inadequacy of the frozen target approximation, 9Ps1H, in this energy range is clear. The large zero energy 9Ps1H S-wave cross section is the result of the small PsH binding energy obtained in this approximation, see Table 2. Consequently, the PsH bound state pole in the scattering amplitude is much closer to zero impact energy than it should be, see Fig. 1, with the result that the cross section rises to too high a value at zero energy. Fig. 2 also illustrates the change in the 9Ps9H cross sections on including the e^+–H^- channel.

Table 4
Electronic spin singlet S-, P- and D-wave phase shifts (in rad) in the 9Ps9H + H^- approximation

Incident momentum (au)	S	P	D
0.1	−0.432	0.221(−1)	0.202(−3)
0.2	−0.833	0.183	0.349(−2)
0.3	−1.179	0.580	0.173(−1)
0.4	−1.466	0.956	0.522(−1)
0.5	−1.699	1.106	0.116
0.6	−1.884	1.134	0.208
0.7	−2.012	1.133	0.324

Powers of 10 are denoted in parentheses.

Fig. 3 shows the same cross sections in the energy range 3.5–6.5 eV. Here we see pronounced resonance structure associated with unstable states of the positron trapped in the field of the H^- ion [9,13]. The 9Ps9H approximation only gives the first of these resonances, and at too high an energy. To see the profound impact of the full resonance structure one needs the 9Ps9H + H^- approximation, i.e. one needs to include the $e^+ + H^-$ channel explicitly in the approximation.

We have fitted the positions and widths of the first few resonances, these are given in Table 5 where comparison is made with the complex coordinate rotation results of Yan and Ho [3,14–16]. We see that the first member of each partial wave series in the 9Ps9H + H^- approximation lies higher in position than the complex coordinate prediction. By contrast, the second member lies lower. Generally speaking, the agreement on positions and widths between the two theoretical results leaves something to be desired.

By combining the electronic spin triplet results in the 9Ps9H approximation from [6] with the present electronic spin singlet results in the 9Ps9H + H^- approximation we have calculated the Ps(1s) + H(1s) total cross section in the energy range 0–6.7 eV, Fig. 4. This cross section shows the spectacular effect of the singlet resonance structures. It should be noted that the cross section of Fig. 4 assumes that the target H atom is spin unpolarized and that no spin analysis is made of the final states [6,9]; the cross section is independent of whether the incident Ps(1s) is ortho or para and, if ortho, of its spin polarization. Partial waves with total angular momentum J from 0 to 4 have been used in calculating the cross section of Fig. 4.

Table 5
Positions and widths (in parentheses) for electronic spin singlet S-, P-, D- and F-wave resonances (in eV)

Resonance	9Ps9H + H$^-$ approximation	Yan and Ho [3,14–16]
S(1)	4.149 (0.103)	4.0058 ± 0.0005 (0.0952 ± 0.0011)
S(2)	4.877 (0.0164)	4.9479 ± 0.0014 (0.0585 ± 0.0027)
S(3)	5.377 (0.0091)	5.3757 ± 0.0054 (0.0435 ± 0.011)
P(1)	4.475 (0.0827)	4.2850 ± 0.0014 (0.0435 ± 0.0027)
P(2)	4.905 (0.0043)	5.0540 ± 0.0027 (0.0585 ± 0.0054)
D(1)	4.899 (0.0872)	4.710 ± 0.0027 (0.0925 ± 0.0054)
D(2)	5.161 (0.0648)	
D(3)	5.496 (0.0328)	
F(1)	5.200 (0.0095)	5.1661 ± 0.0014 (0.0174 ± 0.0027)
F(2)	5.494 (0.0262)	
F(3)	5.661 (0.0294)	

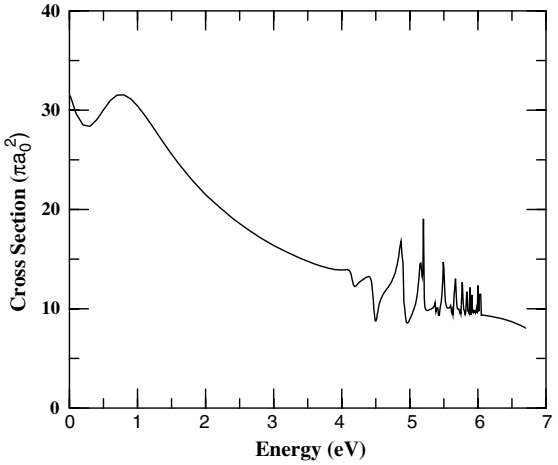

Fig. 4. Total cross section for Ps(1s)–H(1s) scattering.

2.3. Conclusions

It is probably fair to say that we now have a pretty good overall idea of Ps(1s)–H(1s) scattering in the energy range up to 6.7 eV. However, within the context of the coupled pseudostate approach some details remain to be cleared up – the PsH binding energy, the exact details of the resonances, better convergence towards the Kohn variational phase shifts. We speculate that these may be resolved by explicit inclusion of the Ps$^-$ + p channel and, for the resonances, by taking account of the near degeneracy of the e$^+$–H$^-$ and Ps ($n = 3$) channels which all of the approximations used here fail to do (the Ps ($n = 3$) states used here are pseudostates rather than eigenstates, see Table 1). In addition it would be interesting to see what resonance structure might be associated with the Ps$^-$ + p channel. These are matters for future investigation.

3. Positronium scattering by helium (Ps(1s)–He(1^{1}S))

In a large frozen target calculation Blackwood et al. [17] have highlighted significant discrepancies between theory and theory, experiment and experiment and theory and experiment for very low energy o-Ps(1s)–He(1^{1}S) scattering. The work on atomic hydrogen [6] (see Figs. 2 and 5) illustrates nicely the deficiencies of the frozen target approximation at low energies and the need to allow for virtual target excitation. Here we report some new coupled pseudostate calculations for He which relax the frozen target assumption. The generalization of (4) to the case of Ps(1s)–He(1^{1}S) scattering is

$$\Psi = A \sum_{S_A=0,1} \sum_{a,b} \sum_{m} C(1/2, S_A, 1/2, m, -m, 0) \times G_{ab}^{S_A}(\mathbf{R}_1)\phi_a(\mathbf{t}_1)\psi_b^{S_A}(\mathbf{r}_2, \mathbf{r}_3)\zeta_m(s_1)\chi_{-m}^{S_A}(s_2, s_3), \quad (8)$$

where the electron space and spin coordinates are now $(\mathbf{r}_i, s_i)$ $(i = 1, 2, 3)$, ϕ_a is the Ps state, $\zeta_m(s)$ the spin function for the Ps electron with Z-component m, $\psi_b^{S_A}$ is the spatial part of a He state with

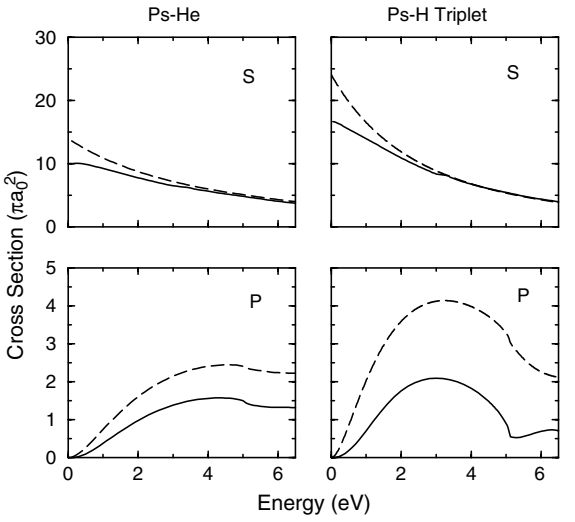

Fig. 5. S- and P-wave cross sections for Ps(1s) elastic scattering by He(1^1S) and H(1s). The H cross sections are for scattering in the electronic spin triplet state. For He: solid curve, 9Ps9He approximation for S-wave and 7Ps7He approximation for P-wave; dashed curve, 9Ps1He approximation for S-wave and 7Ps1He approximation for P-wave. For H: solid curve, 9Ps9H approximation; dashed curve, 9Ps1H approximation.

total electronic spin S_A ($=0$, 1), and $\chi_m^{S_A}$ is the corresponding spin function. Since the total electronic spin of the Ps(1s)–He(1^1S) system is 1/2, the Ps and He states need to be coupled together to give total spin 1/2, that is the purpose of the Clebsch–Gordan Coefficient C in (8). Finally, A is the electron antisymmetrization operator.

We make two approximations on (8). The first is to neglect the He triplet states $S_A = 1$. The second is to approximate the He singlet states in the form

$$\psi_b^{S_A=0}(\mathbf{r}_2, r_3) = N_b(\psi_b(\mathbf{r}_2)\bar{\psi}(r_3) + \psi_b(\mathbf{r}_3)\bar{\psi}(r_2)), \quad (9)$$

where $\bar{\psi}(r)$ is taken to be the He^+(1s) orbital $\sqrt{8/\pi}e^{-2r}$ and N_b is a normalisation constant. The orbitals $\psi_b(\mathbf{r})$ are at our disposal to choose as we see appropriate. The form (9) is the same as that used in the e^+–He scattering calculations of [18]. Using (9) we have constructed 9 He states analogous to the 9H states of Table 1 and labelled as 1^1S, 2^1S, 2^1P, $\overline{3^1\text{S}}$, $\overline{3^1\text{P}}$, $\overline{3^1\text{D}}$, $\overline{4^1\text{S}}$, $\overline{4^1\text{P}}$, $\overline{4^1\text{D}}$. As in Table 1, the $n = 3$ states are constructed so as to sit at the ionization threshold of He(1^1S) at 24.58 eV. The 1^1S, 2^1S and 2^1P states are, of course, now just approximations to the He(1^1S), He(2^1S) and He(2^1P) eigenstates.

Combining the 9 He states described above with the 9 Ps states from Table 1 (a 9Ps9He approximation analogous to 9Ps9H) we have calculated an S-wave Ps(1s)–He(1^1S) elastic scattering cross section in the energy range 0–6.5 eV, Fig. 5. Because we encountered some bad numerical behaviour with the higher partial waves, we have evaluated the P-wave cross section in a reduced approximation, 7Ps7He, in which the Ps and He d-states have been dropped. The P-wave cross section is shown in Fig. 5. Also included in Fig. 5 are the corresponding frozen target cross sections calculated in the 9Ps1He (S-wave) and 7Ps1He (P-wave) approximations. It has been remarked that Ps(1s)–He(1^1S) scattering should be similar to Ps(1s)–H(1s) scattering in the electronic spin triplet state since in both cases antisymmetry keeps the positronium electron and the atomic electron(s) apart, consequently we have added the triplet 9Ps9H and 9Ps1H S- and P-wave cross sections to Fig. 5 for comparison. We see a similar pattern for both H and He which gives us some confidence in our calculations. In each case allowance for virtual target excitation produces a noticeable reduction on the frozen target results. For He this effect seems to be smaller than for H, presumably on account of the higher excitation energies for a He target.

Since the original calculations of Blackwood et al. [17] three other relevant pieces of work have appeared in the literature. In [19] Basu et al. have included both Ps and He excitations in a Ps(1s, 2p) + He(1^1S, 2^1S, 2^1P) coupled eigenstate calculation. They obtain a zero energy elastic cross section of $7.40\pi a_0^2$. This contrasts with our zero energy cross section of $9.9\pi a_0^2$ in the much larger 9Ps9He coupled pseudostate calculation. In [20] Mitroy and Ivanov have used a model potential approximation which yields values for the zero energy cross section ranging from $10.6\pi a_0^2$ to $8.8\pi a_0^2$ depending upon the choice of parameters in the potential. Interestingly, their average cross section of $9.83\pi a_0^2$ agrees well with our present results. Finally, Chiesa et al. [21] have employed the diffusion Monte Carlo method to calculate

S-wave phase shifts in the momentum range 0–0.4 au. They get a zero energy cross section of $7.89\pi a_0^2$.

In Fig. 6 we make a comparison with the low energy experimental data. As discussed in [22], these low energy data, derived from annihilation measurements, correspond to the momentum transfer cross section.

$$\sigma_{\mathrm{mom}} = \int (1 - \cos\theta) \frac{\mathrm{d}\sigma_{\mathrm{el}}}{\mathrm{d}\Omega} \mathrm{d}\Omega, \tag{10}$$

where $\mathrm{d}\sigma_{\mathrm{el}}/\mathrm{d}\Omega$ is the elastic differential cross section and θ is the scattering angle. At zero impact energy where the scattering is all S-wave σ_{mom} is identical with the S-wave total cross section. However, as pointed out in [22], σ_{mom} can diverge rapidly from the total cross section with increasing energy. In Fig. 6 the theoretical results correspond to the momentum transfer cross section. The only exception is the cross section of Chiesa et al. [21] where we have only S-wave data and so the cross section shown is just the S-wave total cross section. The cross section of Basu et al. has been constructed out of the phase shift data given in their paper [19]. Fig. 6 shows that our frozen target approximation agrees well with the experimental point of Nagashima et al. [23]. Our present results are also in agreement with this measurement and close to, but outside, the error bars of the cross sections of Canter et al. [24] and Rytsölä et al. [25]. Most striking, however, is the agreement between these two measurements and the S-wave total cross section of the sophisticated Monte Carlo calculation of Chiesa et al. which, as indicated above, coincides with the momentum transfer cross section at zero energy. Another striking point is the lack of agreement between any of the theories and the cross section of Skalsey et al. [26] centred on 0.725 eV. At this energy our calculations and that of Basu et al. show that σ_{mom} is about 20% smaller than the total cross section, indicating the importance of P-wave scattering. To get agreement with the measurement of Skalsey et al. would require a more spectacular growth in P-wave scattering.

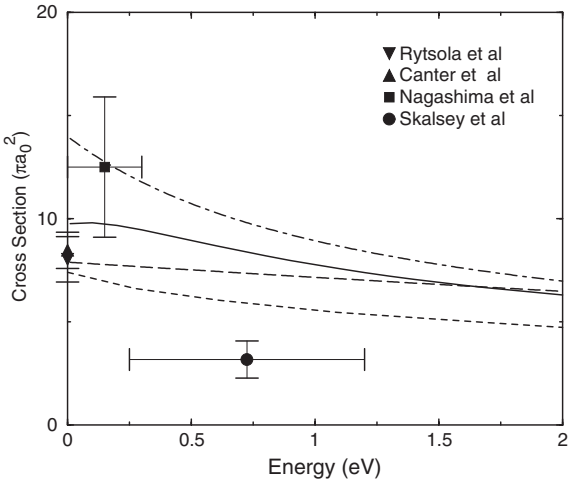

Fig. 6. Momentum transfer cross sections for Ps(1s) + He(1^1S) scattering. Theory: solid curve, present results with 9Ps9He approximation for S-wave and 7Ps7He approximation for P-wave; dash–dot curve, frozen target results with 9Ps1He approximation for S-wave and 7Ps1He approximation for P-wave; long-dashed curve, S-wave total cross section of Chiesa et al. [21]; short-dashed curve, cross section of Basu et al. [19]. Experiment: square, Nagashima et al. [23]; up triangle, Canter et al. [24]; down triangle, Rytsölä et al. [25]; circle, Skalsey et al. [26].

There are a number of ways in which the present calculations can be improved. Firstly, there is a need to eliminate any doubts concerning the use of an approximation to the He ground state wave function, see (9). Secondly, there is the question of the importance of He triplet states in the expansion (8). Finally, we have remarked upon the similarity of Ps(1s)–He(1^1S) scattering and Ps(1s)–H(1s) triplet scattering, see Fig. 5, but there is one mechanism in Ps(1s)–He(1^1S) scattering which is not available to the Ps(1s)–H(1s) triplet case, that mechanism is Ps^- formation ($Ps(1s) + He(1^1S) \Rightarrow Ps^- + He^+(1s)$) [27]. This might be a more important mechanism than has been realised and may, perhaps, resolve the discrepancy between theory and the experiment of Skalsey et al. [26]. In addition, this mechanism would be a possible source of resonances in Ps(1s)–He(1^1S) scattering although the resonance structure may be small in magnitude.

4. Positronium scattering by lithium (Ps(1s)–Li(2s))

Alkali metals behave in many respects like a one-electron system in which the single valence

electron revolves outside a frozen core. A priori, one might therefore think that Ps–alkali scattering would be similar to Ps–H scattering. That this is not so is suggested by the event line for Ps(1s)–Li(2s) scattering shown in Fig. 7. Compared with Fig. 1 for Ps(1s)–H(1s), everything is "reversed". Yes, there is a bound state of Ps and Li [28] analogous to PsH, but with increasing energy it is atom excitation and ionization that precede Ps excitation and ionization, the opposite of Fig. 1. We also see that the order of Ps^- and Li^- formation is reversed compared to that of Ps^- and H^- formation shown in Fig. 1. Ps^- formation presumably therefore plays a much more prominent role for the alkali systems than for H, and, in particular, with regard to resonance formation.

An interesting feature which Fig. 1 does not possess is a channel corresponding to the formation of a bound state of the positron with the atom, in Fig. 7 the $e^- + Lie^+$ channel. The binding energy of positronic lithium, as Lie^+ is called, is very small and the threshold for this channel (at 5.326 eV) is almost degenerate with that for ionization of the Li atom (at 5.392 eV), lying only 0.066 eV below [29]. Again, a priori, one would expect Rydberg resonance structure associated with this channel, but of what amplitude is hard to predict. Unlike the $Ps^- + Li^+$ and $e^+ + Li^-$ channels which also promise Rydberg resonance structure but only in electronic spin singlet scattering, the positronic lithium channel couples to both electronic spin singlet and electronic spin triplet scattering.

We are unable at this point to execute an approximation which does justice to Fig. 7. Rather, we have elected for a simple coupled eigenstate approximation to get a rough feeling of how things might go. Earlier coupled eigenstate calculations have been published by Ray [30], Biswas [31] and Chakraborty et al. [32], but in all cases either the Ps or the Li atom has been frozen in its ground state. Here we publish the first calculations which allow for excitation of both the Ps and the Li atom.

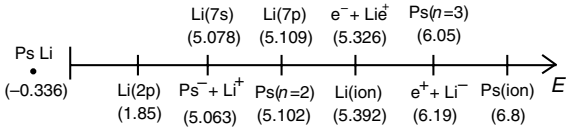

Fig. 7. Event line for Ps(1s)–Li(2s) scattering in the electronic spin singlet state. Events are shown as a function of the impact energy E (in eV). The diagram is purely schematic and not to scale. For scattering in the electronic spin triplet state, the PsLi bound state and the $Ps^- + Li^+$ and $e^+ + Li^-$ formation channels should be omitted.

Our approximation is Ps(1s, 2s, 2p) + Li(2s, 2p). We have constructed the Li(2s) and Li(2p) valence orbitals using the model potential of Stein [33]. The collision formulation is the same as that given in Eqs. (1)–(6) of Section 2.2 for Ps–H, except that we also include potentials $V_p(r_p)$ and $-V_e(r_i)$ to allow for the interaction of the positron and the electrons with the frozen $1s^2$ core of the Li atom [34]. Our approximation contains a representation of the van der Waals interaction, $-C_6/R^6$, with $C_6 = 288$ au. In a much larger calculation of C_6 using pseudostates for the Ps but keeping just the Li(2s) and Li(2p) states, we get $C_6 = 451$ au. The present coupled eigenstate calculation therefore includes about 60% of the full van der Waals effect. For Ps(1s)–H(1s), $C_6 = 34.8$ au [6]. The van der Waals force is therefore an order of magnitude stronger for Ps interacting with Li. Our approximation gives a PsLi bound state with binding energy 0.224 eV, somewhat less than 0.336 eV, the most accurate calculated value [28].

Fig. 8 shows our calculated total cross section and its components. We have assumed that the Li atom is spin unpolarized and that final state spins are not resolved, the cross section is then 1/4 times singlet plus 3/4 times triplet [6]. Our results apply either for o-Ps or p-Ps scattering and are independent of any spin polarization of the o-Ps [6]. From Fig. 8 we see that at very low energies we can expect an elastic cross section of the order of $100\pi a_0^2$, the spin singlet component of this cross section is much larger as a result of the small binding energy of the PsLi pole in the singlet scattering amplitude. To get the zero energy cross section right is going to require an approximation with an accurate representation of the PsLi binding. Away from threshold the elastic cross section falls rapidly but then, with the opening of the Li(2p) channel at 1.85 eV (Fig. 7), it experiences a

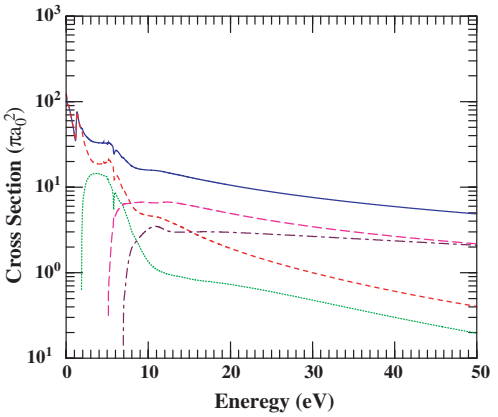

Fig. 8. Cross sections for Ps(1s) scattering by Li(2s) as calculated in the Ps(1s, 2s, 2p) + Li(2s, 2p) approximation. Curves: solid, total cross section; short-dashed, elastic; dotted, Ps(1s) + Li(2p); long-dashed, Ps ($n = 2$) + Li(2s); dash–dot, Ps ($n = 2$) + Li(2p).

sudden rise resulting in a pronounced structure. The $\mathrm{Ps}(1s) + \mathrm{Li}(2s) \Rightarrow \mathrm{Ps}(1s) + \mathrm{Li}(2p)$ cross section increases rapidly from threshold, reaches a maximum of $17\pi a_0^2$ at 2.1 eV, then quickly turns over and, comparatively speaking, is negligible beyond 10 eV. Beyond 8 eV the $\mathrm{Ps}(1s) + \mathrm{Li}(2s) \Rightarrow \mathrm{Ps}\ (n = 2) + \mathrm{Li}(2s)$ cross section is dominant. The opening of this channel leads to structure in the other open channels near 5.1 eV. By 50 eV the double excitation cross section $\mathrm{Ps}(1s) + \mathrm{Li}(2s) \Rightarrow \mathrm{Ps}\ (n = 2) + \mathrm{Li}(2p)$ has risen to meet the Ps $(n = 2) + \mathrm{Li}(2s)$ curve. The importance of double excitation at high energies is not surprising [35]. Our model predicts that Ps $(n = 2)$ excitation, irrespective of the final state of the Li atom, will be dominant at high energies. However, we should not accept that, in reality, this will be so. We suspect that, in a more realistic treatment allowing for ionization of the Ps, it will, as in other cases [5,6,17,22], be Ps ionization which is dominant at high energies with Ps $(n = 2)$ discrete excitation being much less significant. The problem is that, in the present model, there is nowhere for Ps excitation to go but into the Ps $(n = 2)$ channels. Ps excitation which otherwise would flow into ionization is possibly being deflected into the Ps $(n = 2)$ channels. Clearly a more detailed calculation is required.

5. Conclusions

We have presented new coupled state calculations for Ps(1s) scattering by H(1s) in the electronic spin singlet state, by $\mathrm{He}(1^1S)$ at very low energies, and by Li(2s). One interesting theme that emerges from all three cases is the question of the importance of Ps^- formation, whether real or virtual. For Ps(1s)–H(1s) scattering we speculate that the inclusion of virtual Ps^- formation may be necessary to tune the calculations into agreement with the accurate variational results of Van Reeth and Humberston [12] and with accurate bound state calculations of PsH binding [3]. For Ps(1s)–$\mathrm{He}(1^1S)$ scattering, virtual Ps^- formation in the reaction $\mathrm{Ps}(1s) + \mathrm{He}(1^1S) \Rightarrow \mathrm{Ps}^- + \mathrm{He}^+(1s)$ provides us with a mechanism for breaking away from the pattern of Ps(1s)–H(1s) triplet scattering which present coupled state calculations on He seem to follow, and perhaps a route to agreement with the seemingly anomalous experimental result of Skalsey et al. [26], Fig. 6. For Ps(1s) scattering by Li(2s), or indeed any alkali, we have, because of the energetics, the very interesting possibility that Ps^- formation, both real and virtual, may play a much more profound role than had ever been envisaged. Clearly the study of Ps^- formation is an important direction for future research.

For Ps(1s)–H(1s) scattering another interesting feature which so far has not been properly treated, is the near degeneracy of the Ps $(n = 3)$ excitation channels and the H^- formation channel, this must surely have some significant effect on the resonance structure associated with the H^- threshold. For Ps(1s)–$\mathrm{He}(1^1S)$ scattering there is a need to know about sensitivity to the use of approximate $\mathrm{He}(1^1S)$ target wave functions, as well as the role of He triplet states in the collisional wave function expansion (8). For Ps(1s)–alkali scattering most of the really interesting physics would seem to lie at impact energies below 10 eV, which is a challenge to experimentalists. The challenge to theory in this case is to represent the Ps^- and alkali negative ion channels, and to a lesser extent the positronic lithium channel, as well as the Ps and alkali atom channels. Without an adequate description of the ion channels it is unlikely that an accurate calculation of resonances can be made [31]. Also,

because of the small binding energies of Ps–alkali bound states [28] and their role as poles in the scattering amplitude, near threshold electronic spin singlet cross sections for Ps(1s)–alkali scattering will be very large and very sensitive to the pole position. Consequently, any realistic treatment of Ps(1s)–alkali scattering at low energies will need to incorporate a reasonably accurate representation of the Ps–alkali bound state.

Acknowledgements

This research was supported by EPSRC grants GR/N07424 and GR/R83118/01. We are also greatly indebted to Prof. T. Koga for supplying us with the accurate H^- wave function.

References

[1] P.J. Mohr, B.N. Taylor, Rev. Mod. Phys. 72 (2000) 351.
[2] A. Ore, Phys. Rev. 83 (1951) 665.
[3] Z.-C. Yan, Y.K. Ho, Phys. Rev. A 59 (1999) 2697.
[4] A.M. Frolov, V.H. Smith Jr., Phys. Rev. A 49 (1994) 3580.
[5] C.P. Campbell, M.T. McAlinden, F.G.R.S. MacDonald, H.R.J. Walters, Phys. Rev. Lett. 80 (1998) 5097.
[6] J.E. Blackwood, M.T. McAlinden, H.R.J. Walters, Phys. Rev. A 65 (2002) 032517.
[7] P.G. Burke, W.D. Robb, Adv. At. Mol. Phys. 11 (1975) 143.
[8] A.A. Kernoghan, M.T. McAlinden, H.R.J. Walters, J. Phys. B 28 (1995) 1079.
[9] J.E. Blackwood, M.T. McAlinden, H.R.J. Walters, Phys. Rev. A 65 (2002) 030502.
[10] T. Kinoshita, Phys. Rev. 105 (1957) 1490.
[11] T. Koga, private communication.
[12] P. Van Reeth, J.W. Humberston, J. Phys. B 36 (2003) 1923.
[13] R.J. Drachman, Phys. Rev. A 19 (1979) 1900.
[14] Z.-C. Yan, Y.K. Ho, Phys. Rev. A 57 (1998) R2270.
[15] Y.K. Ho, Z.-C. Yan, J. Phys. B 31 (1998) L877.
[16] Y.K. Ho, Z.-C. Yan, Phys. Rev. A 62 (2000) 052503.
[17] J.E. Blackwood, C.P. Campbell, M.T. McAlinden, H.R.J. Walters, Phys. Rev. A 60 (1999) 4454.
[18] C.P. Campbell, M.T. McAlinden, A.A. Kernoghan, H.R.J. Walters, Nucl. Instr. and Meth. B 143 (1998) 41.
[19] A. Basu, P.K. Sinha, A.S. Ghosh, Phys. Rev. A 63 (2001) 052503.
[20] J. Mitroy, I.A. Ivanov, Phys. Rev. A 65 (2002) 012509.
[21] S. Chiesa, M. Mella, G. Morosi, Phys. Rev. A 66 (2002) 042502.
[22] J.E. Blackwood, M.T. McAlinden, H.R.J. Walters, J. Phys. B 35 (2002) 2661.
[23] Y. Nagashima, T. Hyodo, F. Fujiwara, A. Ichimura, J. Phys. B 31 (1998) 329.
[24] K.F. Canter, J.D. McNutt, L.O. Roellig, Phys. Rev. A 12 (1975) 375.
[25] K. Rytsölä, J. Vettenranta, P. Hautojärvi, J. Phys. B 17 (1984) 3359.
[26] M. Skalsey, J.J. Engbrecht, C.M. Nakamura, R.S. Vallery, D.W. Gidley, Phys. Rev. A 67 (2003) 022504.
[27] H.R.J. Walters, J.E. Blackwood, M.T. McAlinden, in: C.M. Surko, F.A. Gianturco (Eds.), New Directions in Antimatter Chemistry and Physics, Kluwer, Dordrecht, 2001, p. 173.
[28] J. Mitroy, G.G. Ryzhikh, J. Phys. B 34 (2001) 2001.
[29] G.G. Ryzhikh, J. Mitroy, K. Varga, J. Phys. B 31 (1998) 3965.
[30] H. Ray, J. Phys. B 32 (1999) 5681;
J. Phys. B 33 (2000) 4285;
J. Phys. B 35 (2002) 2625.
[31] P.K. Biswas, Phys. Rev. A 61 (2000) 012502.
[32] A. Chakraborty, P.K. Sinha, A.S. Ghosh, Phys. Rev. A 65 (2002) 062504.
[33] M. Stein, J. Phys. B 26 (1993) 2087.
[34] A.C.H. Yu, Thesis, The Queen's University of Belfast, 2003.
[35] M.T. McAlinden, F.G.R.S. MacDonald, H.R.J. Walters, Can. J. Phys. 74 (1996) 434.